Received: 14 September 2022 | Accepted: 11 December 2022

DOI: 10.1111/1462-2920.16326

RESEARCH ARTICLE

ENVIRONMENTAL MICROBIOLOGY Applied Microbiology International

Growth dynamics and transcriptional responses of a Red Sea *Prochlorococcus* strain to varying temperatures

Abbrar Labban[1,2] | **Ahmed A. Shibl**[3,4] | **Maria Ll. Calleja**[5] | **Pei-Ying Hong**[2] | **Xosé Anxelu G. Morán**[1,6]

[1]Marine Science, Biological and Environmental Science and Engineering Division, King Abdullah University of Science and Technology (KAUST), Thuwal, Kingdom of Saudi Arabia

[2]Environmental Science and Engineering, Biological and Environmental Science and Engineering Division, King Abdullah University of Science and Technology (KAUST), Thuwal, Kingdom of Saudi Arabia

[3]Genetic Heritage Group, Biology Program, New York University Abu Dhabi, Abu Dhabi, United Arab Emirates

[4]Public Health Research Center, New York University Abu Dhabi, Abu Dhabi, United Arab Emirates

[5]Climate Geochemistry Department, Max Plank Institute for Chemistry, Mainz, Germany

[6]Centro Oceanográfico de Gijón/Xixón, Instituto Español de Oceanografía (IEO-CSIC), Gijón/Xixón, Spain

Correspondence
Xosé Anxelu G. Morán, Marine Science, Biological and Environmental Science and Engineering Division, 4700 King Abdullah University of Science and Technology (KAUST), Thuwal 23955-6900, Kingdom of Saudi Arabia.
Email: xelu.moran@kaust.edu.sa xelu.moran@ieo.csic.es

Funding information
King Abdullah University of Science and Technology

Abstract

Prochlorococcus play a crucial role in the ocean's biogeochemical cycling, but it remains controversial how they will respond to global warming. Here we assessed the response to temperature (22–30°C) of the growth dynamics and gene expression profiles of a Red Sea *Prochlorococcus* strain (RSP50) in a non-axenic culture. Both the specific growth rate (0.55–0.80 day^{-1}) and cell size (0.04–0.07 μm^3) of *Prochlorococcus* increased significantly with temperature. The primary production released extracellularly ranged from 20% to 34%, with humic-like fluorescent compounds increasing up to fivefold as *Prochlorococcus* reached its maximum abundance. At 30°C, genes involved in carbon fixation such as CsoS2 and CsoS3 and photosynthetic electron transport including PTOX were downregulated, suggesting a cellular homeostasis and energy saving mechanism response. In contrast, PTOX was found upregulated at 22°C and 24°C. Similar results were found for transaldolase, related to carbon metabolism, and citrate synthase, an important enzyme in the TCA cycle. Our data suggest that in spite of the currently warm temperatures of the Red Sea, *Prochlorococcus* can modulate its gene expression profiles to permit growth at temperatures lower than its optimum temperature (28°C) but is unable to cope with temperatures exceeding 30°C.

INTRODUCTION

The genus *Prochlorococcus* plays an essential role in marine planktonic communities, contributing significantly to total photosynthetic biomass and productivity, especially in the oligotrophic ocean (Geider et al., 2014; Partensky et al., 1999). Given its prevailing role as primary producer, the dissolved organic matter (DOM) released by *Prochlorococcus* is an essential source for heterotrophic bacterioplankton in tropical and subtropical waters (Bertilsson et al., 2005). *Prochlorococcus* is the most abundant (Flombaum et al., 2013; Partensky et al., 1999) and smallest marine photosynthetic organism, with a cell diameter typically ranging from 0.5 to 0.7 μm (Morel et al., 1993). *Prochlorococcus* consists of many genetically and physiologically distinct clades, grouped as either high-light (HL) or low-light (LL)-adapted ecotypes (Moore et al., 1995; Moore et al., 1998; Moore & Chisholm, 1999; Ting et al., 2002). The distribution patterns of *Prochlorococcus* differ according to environmental gradients (Biller et al., 2015; Partensky et al., 1999; Scanlan et al., 2009). Among the physicochemical factors, temperature, exposure to light and

nutrients concentrations are the major drivers in shaping the differential distributions of *Prochlorococcus* in the oceans (Johnson et al., 2006; Scanlan et al., 2009). Surface waters are generally dominated by HL-adapted cells while LL-adapted cells are restricted mostly to deeper levels within the euphotic zone (Rocap et al., 2002; West & Scanlan, 1999). Regardless of the ecotype, high *Prochlorococcus* abundances are usually associated with oligotrophic environments, highly stable water columns (Lindell & Post, 1995), and warm temperatures (Bouman et al., 2006; Partensky et al., 1999).

Temperature is a key regulator of phytoplankton metabolic processes (Raven & Geider, 1988) and determines the biogeographical borders of major phytoplankton groups (Needoba et al., 2007). Global warming can affect the metabolism of planktonic microbes either directly, resulting in changes in their distribution, phenology and cell size (Daufresne et al., 2009), or indirectly by e.g. enhancing water column stratification (Coma et al., 2009; Doney et al., 2012). The spatial and temporal extension of strongly stratified water columns will reduce new nutrient inputs from deep waters, making vast regions become more oligotrophic, overall likely increasing the predominance of *Prochlorococcus* (Flombaum et al., 2013) and also re-arranging the local distribution of their ecotypes (Biller et al., 2015). Using a modelling approach, the abundance of *Prochlorococcus* is predicted to moderately increase (Agusti et al., 2019) and extend towards the poles as the temperature of the oceans rises (Flombaum et al., 2013).

The Red Sea, subjected to very high temperatures and salinities (Berumen et al., 2019; Rasul et al., 2015; Sofianos & Johns, 2007), represents a unique oligotrophic environment (Raitsos et al., 2013) for assessing how tropical *Prochlorococcus* will respond to global warming. The surface waters down to ca. 50 m of the Red Sea are dominated by HL-adapted *Prochlorococcus*, mostly belonging to the HLII group (Fuller et al., 2005; Ngugi et al., 2012; Shibl et al., 2014; Shibl et al., 2016). One such strain was isolated from the main basin (22.64° N and 38.49° E, 10 m) and named as RSP50 (Shibl et al., 2018). From its isolation in a sea that naturally experiences some of the warmest seawater temperatures on earth, we might expect *Prochlorococcus* RSP50 to be well adapted to high temperatures. However, insufficient in situ observations or experimental assessments currently preclude us from concluding how future temperature regimes of the Red Sea will affect *Prochlorococcus* populations.

Here, we report on the growth dynamics and transcriptomic responses of a non-axenic culture of *Prochlorococcus* RSP50 acclimated to five different temperatures covering the natural range of the central Red Sea (22–30°C). The culture was non-axenic on purpose. First, it is challenging to culture and maintain it pure (Morris et al., 2008; Morris et al., 2011) and second, co-culturing *Prochlorococcus* with heterotrophic bacteria has been shown to increase their tolerance to temperature stress (Ma et al., 2017). To that end, we monitored the abundance, cell size, carbon and chlorophyll *a* content of *Prochlorococcus* RSP50, as well as the concentration and optical properties including fluorescence of the dissolved organic matter (DOM) present in the co-cultures until cyanobacteria reached their maximum cell abundance. RNA-sequencing was performed during the exponential growth phase of RSP50. Assessing the growth and transcriptional responses to temperature of a Red Sea model *Prochlorococcus* can contribute to a meaningful assessment of how rate-limiting temperatures may impact these crucial players in biogeochemical cycles.

RESULTS

Growth dynamics and cell size responses of *Prochlorococcus* RSP50 to temperature

After acclimation to the five temperatures tested, *Prochlorococcus* RSP50 grew exponentially for 8–11 days (Figure S1). Carrying capacities (i.e. maximum abundances) were reached earlier at warmer temperatures but showed rather constant values ($2.9 \pm 0.2 \times 10^8$ cells mL^{-1}). Specific growth rates (μ) of the RSP50 strain based on changes in cell abundance (Figure S1) clearly increased from 22°C to 28°C and decreased at 30°C, although it started to reach a plateau at 26°C (Figure 1A). Values ranged from 0.55 to 0.80 day^{-1} and were strongly and positively correlated with temperature ($r = 0.91$, p-value <0.00001, $n = 16$, excluding the 30°C value). Similarly, chlorophyll *a*-based growth rates (0.42–0.66 day^{-1}) increased with temperature and peaked at 28°C (Figure 1B), following the same pattern as the specific growth rates shown in Figure 1A ($r = 0.88$ with temperature, p-value <0.00001, $n = 16$, excluding the 30°C values). The corresponding carbon-to-chlorophyll *a* ratio (C:Chl *a*) using actual cell size changes (see below) ranged from 12.6 to 18.5, with the maximum value found at 30°C (Figure S3).

Mean cell sizes of *Prochlorococcus* ranged from 0.04 to 0.07 μm^3 (Figure 2) and were positively correlated with temperature throughout the whole experimental range ($r = 0.87$, p-value <0.00001, $n = 20$), that is, although the specific growth rate reached its maximum value at 28°C, RSP50 cell size peaked at 30°C.

Dissolved organic matter dynamics associated to *Prochlorococcus* RSP50 growth

We monitored the carbon concentration and selected properties of the dissolved organic compounds released by *Prochlorococcus* to the culture medium during their growth. The initial DOC concentration in the cultures was

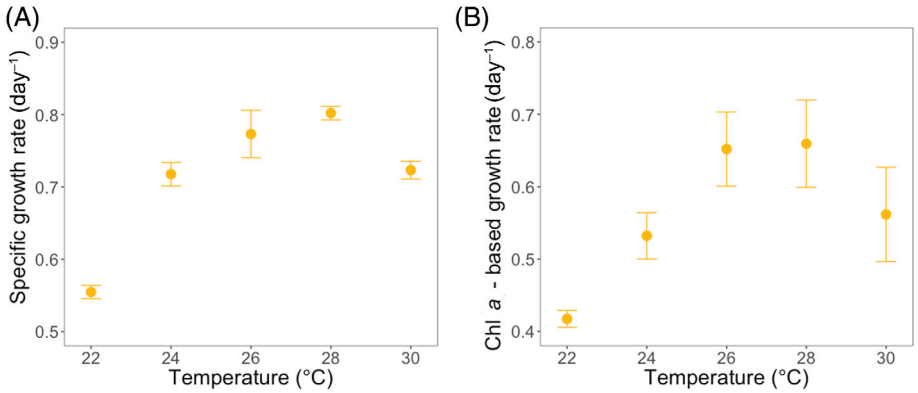

FIGURE 1 Mean growth rates of *Prochlorococcus* RSP50 versus incubation temperature using flow cytometrically-determined cell abundances measured daily (A) and chlorophyll *a* (Chl *a*) concentrations measured 3 times during exponential growth (B). Error bars represent standard deviations.

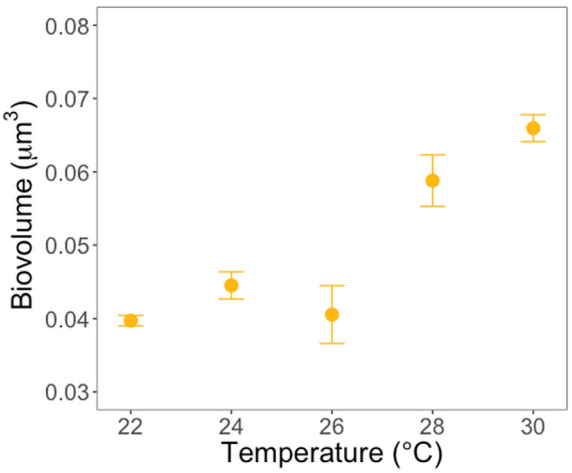

FIGURE 2 Mean cell sizes of *Prochlorococcus* RSP50 vs. incubation temperature. Error bars represent standard deviations.

110.1 ± 10.6 µmol C L^{-1}. Over the course of the experiment, a net increase in DOC concentration was observed at all temperatures except at 22°C (Table 1) and the magnitude of the increase was higher at warmer temperatures. DOC concentration showed mean percentage increases of 35%, 49%, 52%, and 58% at 24°C, 26°C, 28°C, and 30°C, respectively, relative to the initial values by the end of the incubations (Figure S4).

Coloured dissolved organic matter or CDOM is the fraction of DOM that absorbs light in the UV and visible spectra. The absorbance spectra at the end of the incubations differed from those of the initial CDOM (Figure S5). As expected, CDOM absorbed largely in the UV side of the spectra, and absorption increased with DOC concentration. A ubiquitous peak of maximum absorbance was observed at the end of all incubations at 445 nm (Figure S5), in accordance with the absorption maxima of intact *Prochlorococcus* cells previously reported (Morel et al., 1993). Using PARAFAC-EEM analysis, a model of 4 fluorescent components was validated. The four validated peaks are: Peak C1 at $Ex_1(Ex_2)$/Em 252(321)/392 nm; peak C2 Ex/Em 273/297; peak C3 $Ex_1(Ex_2)$/Em 255(381)/457 nm; and peak C4 Ex/Em 282/337 (Figure 3). C1 and C3 have humic-like fluorescent characteristics while C2 and C4 show protein-like fluorescent features (Figure 3).

The changes in the fluorescent signal of all four components with time for each temperature treatment are shown in Figure S6 (left panels). Total fluorescence and changes in the relative abundance of each component are also shown for each sampling time (Figure S6, right panels). Although all components increased with time, C2 was the most abundant fluorescent component while C3 was the less abundant at any given temperature during the first half of all incubations (Figure S6). However, peak C2 remained notably more abundant than the other components only in the cultures kept at 22°C at the end of the incubation (Figure S6). None of the components showed any significant correlation with increasing temperature at the initial time or during *Prochlorococcus* growth (i.e. during the first 9, 7 and 6 incubation days at the 22, 24 and 26–30°C cultures respectively, Figure S6). Only at the maximum abundance of *Prochlorococcus* (i.e., days 11, 9 and 8 of cultures at 22°C, 24°C and 26–30°C respectively, Figure S1 and S6), C1 and C3 increased strongly with temperature ($r = 0.92$, p-value <0.00001 and $r = 0.86$, p-value <0.00001, respectively, $n = 20$), with C4 showing a less strong though significant response ($r = 0.63$, p-value $= 0.003$, $n = 20$). C2 did not show any significant pattern with temperature. The relative abundance of fluorescent protein-like components (C2 + C4) decreased in all treatments, except at 22°C (Figure S7). As a consequence, the protein to humic fluorescence ratio (PROT/HUM, calculated as the sum of fluorescence emitted by the protein-like components, C2 and C4, divided by that of the humic-like components, C1 and C3), decreased in all incubations (down to 40%), except at the 22°C treatment, mirroring the pattern observed for DOC concentration changes (Figure S4).

TABLE 1 Mean ± SD values of dissolved organic matter measured in the temperature-acclimated *Prochlorococcus* RSP50 cultures at the onset (DOM initial) and end (DOM final) of the incubations. Both absolute (DOC, μmol L^{-1}) and normalized to cyanobacteria biomass (DOC_{norm}, μmol μg *Prochlorococcus* $^{-1}$) DOC concentrations are shown, together with the fluorescence intensity (Raman units or R.U.) of the four identified FDOM components.

	DOM initial						DOM final					
			Humic-like components		Protein-like components				Humic-like components		Protein-like components	
Temperature	DOC	DOC_{norm}	Peak C1	Peak C3	Peak C2	Peak C4	DOC	DOC_{norm}	Peak C1	Peak C3	Peak C2	Peak C4
22°C	122.0 ± 6.1	50.86 ± 51.00	0.060 ± 0.007	0.030 ± 0.012	0.086 ± 0.012	0.037 ± 0.011	116.1 ± 18.3	0.36 ± 0.59	0.111 ± 0.003	0.099 ± 0.009	0.211 ± 0.019	0.129 ± 0.020
24°C	113.0 ± 3.8	9.24 ± 1.50	0.048 ± 0.002	0.016 ± 0.003	0.080 ± 0.002	0.025 ± 0.002	152.6 ± 8.4	0.08 ± 0.02	0.163 ± 0.019	0.123 ± 0.015	0.190 ± 0.012	0.180 ± 0.020
26°C	111.8 ± 2.4	10.92 ± 0.60	0.044 ± 0.001	0.014 ± 0.001	0.083 ± 0.005	0.025 ± 0.003	166.9 ± 55.6	0.08 ± 0.01	0.152 ± 0.019	0.118 ± 0.019	0.194 ± 0.038	0.162 ± 0.064
28°C	90.6 ± 3.3	6.11 ± 1.93	0.043 ± 0.002	0.031 ± 0.021	0.093 ± 0.010	0.029 ± 0.003	137.8 ± 1.9	0.04 ± 0.00	0.229 ± 0.014	0.169 ± 0.018	0.195 ± 0.030	0.204 ± 0.038
30°C	113.0 ± 27.4	4.10 ± 1.03	0.066 ± 0.008	0.026 ± 0.008	0.102 ± 0.023	0.054 ± 0.025	178.9 ± 66.9	0.20 ± 0.31	0.258 ± 0.019	0.180 ± 0.013	0.268 ± 0.028	0.226 ± 0.030

The increase in RSP50 biomass during the course of the incubation can be considered as an estimation of particulate primary production (PPP). PPP ranged from 105 to 389 μg C L^{-1} day^{-1} and increased significantly with temperature within the experimental range ($r = 0.96$, p-value $= 0.009$, $n = 5$), although it declined slightly at 30°C (378 μg C L^{-1} day^{-1}, Table 2). We also estimated the rates of dissolved primary production (DPP) based on the changes in DOC measured over the course of the incubations. However, these values should be considered net DPP since heterotrophic bacteria, which as expected grew consistently in the non-axenic cultures, also contributed to DOC fluxes by taking it up to meet their metabolic requirements. Bacterial heterotrophic production (BHP) ranged from 7.9 to 25.6 μg C L^{-1} day^{-1}, at 22°C and 30°C, respectively (Table 2), equivalent to 19%–35% of the measured net DPP. BHP only considers the amount of consumed DOC that was transformed into bacterial biomass, while a larger fraction is of DOC taken up is typically respired. By applying literature values of bacterial growth efficiency (BGE) we can however estimate the total demand of carbon needed to support the observed BHP or bacterial carbon demand (BCD = BHP/BGE). We used a conservative BGE value of 30% for heterotrophic bacteria growing in a nutrient-rich environment (del Giorgio & Cole 1998) in order to estimate BCD. Finally, we added the calculated BCD values to estimate the gross (i.e. total) DPP at each temperature. Gross DPP roughly doubled the net DPP values (except at 22°C, where virtually no accumulation of DOC was detected), ranging from 27 to 193 μg C L^{-1} day^{-1} (Table 2). The same as PPP, both net and gross DPP values were also strongly correlated with incubation temperature ($r = 0.93$ and 0.90, $p = 0.008$ and 0.014, respectively, $n = 5$). Consequently, the variance in *Prochlorococcus* RSP50 total primary production (TPP, i.e. the sum of PPP and gross DPP, Table 2) could almost be fully explained by incubation temperature ($r = 0.99$, $p = 0.002$, $n = 5$). The amount of TPP that is released as dissolved compounds is known as percent extracellular release (PER = DPP/TPP × 100), which ranged from 20.3% to 33.8% in our culture (Table 2). Although its positive correlation with temperature was not significant ($r = 0.65$, $p = 0.237$, $n = 5$), PER at 30°C was notably higher than at the optimal growth temperature of 28°C.

Transcriptomic responses of *Prochlorococcus* RSP50 to temperature

Since 28°C was the optimal temperature for growth, differential gene expression of the RSP50 strain at the remaining temperatures was assessed against it. The highest number of upregulated genes was found at 22°C (31 genes), followed by 24°C (30 genes), and

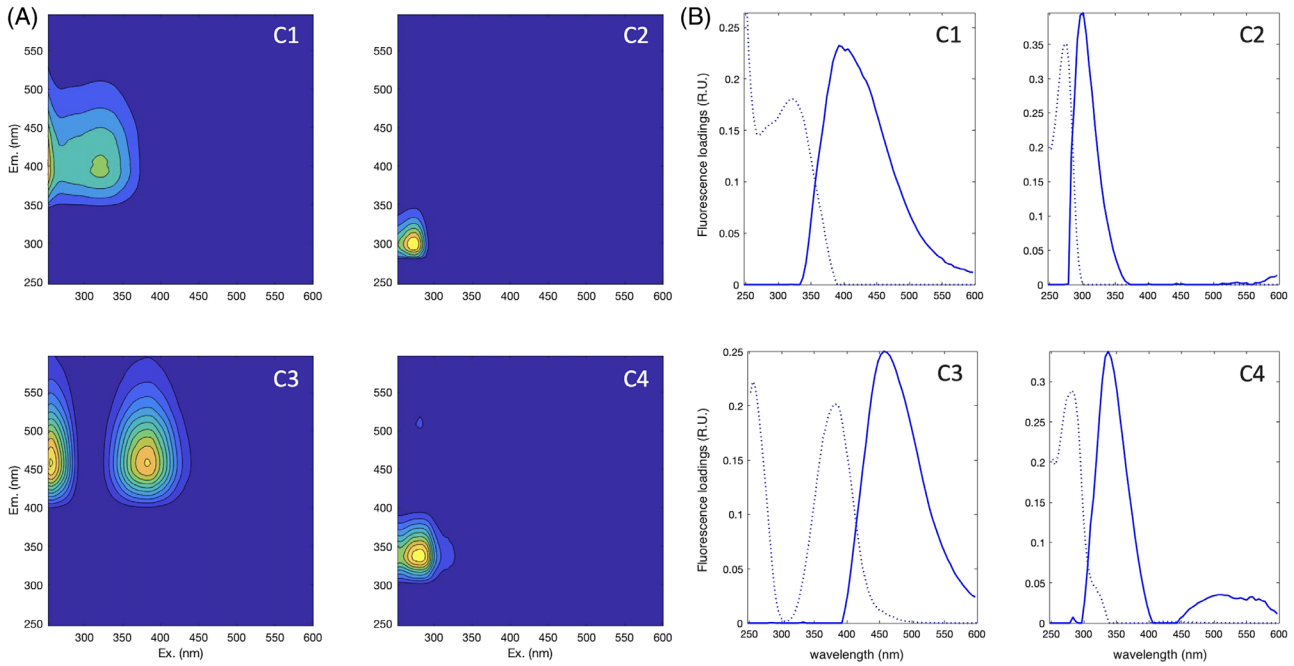

FIGURE 3 (A) Fluorescence matrices of the 4 identified PARAFAC FDOM components released by *Prochlorococcus* RSP50 cultures. See the text for details. (B) Excitation (grey dotted lines) and emissions (blue lines) fluorescence intensities of the four components.

TABLE 2 Mean particulate primary production (PPP) and dissolved primary production (DPP), both measured (net) and estimated (gross), in the *Prochlorococcus* RSP50 cultures at the five different temperatures

Temperature (°C)	PPP	Net DPP	Gross DPP	BHP	TPP	PER (%)
		(μg C L^{-1} day^{-1})				
22	104.5 (52.6)	0.4 (0)[a]	26.6	7.9 (0.5)	131.1	20.3
24	197.3 (30.4)	34.9 (16.9)	75.5	12.2 (2.6)	272.9	27.7
26	239.1 (49.1)	48.7 (63.5)	78.7	9.0 (2.8)	317.8	24.8
28	389.2 (19.1)	57.8 (7.3)	111.8	16.2 (1.8)	500.9	22.3
30	377.6 (210.8)	107.2 (93.0)[b]	192.5	25.6 (8.7)	570.1	33.8

Note: Gross DPP was calculated taking into account the increase in heterotrophic bacteria biomass or bacterial heterotrophic production (BHP) and a bacterial growth efficiency of 30% (see the text for details). Total primary production (PPP + DPP) was calculated with gross DPP values, the same as the percent extracellular release (PER = DPP/TPP). Values among parentheses are SD.

[a]Only one valid replicate.

[b]Mean and SD of three replicates.

30°C (18 genes) while no genes were significantly upregulated at 26°C (Table S1, Figures S8 and S9). The number of downregulated genes peaked at 22°C (121 genes), followed by 30°C (28 genes), 26°C (22 genes) and 24°C (17 genes) (Table S1, Figures S8 and S9).

Photosynthesis by *Prochlorococcus* RSP50 seemed to be affected at non-optimal growth temperatures. For example, the gene BSR22_00119 encoding the chlorophyll *a-b* binding light harvesting protein PcbD, involved in collecting and transferring light energy to photosystems I and II, was down regulated by a − 1.4 $\log_2$ fold change at 26°C while it was highly downregulated, with −3 and − 2.3 $\log_2$ fold changes, at the extreme low (22°C) and high (30°C) temperatures, respectively (Figure 4). Two genes related to photosynthetic electron transfers were downregulated at 22°C only; BSR22_00120 encoding flavodoxin and BSR22_01699 encoding a rieske iron–sulfur protein 2Fe–2S subunit (Figure 4). Two genes specific to photosystem I, BSR22_00498 encoding subunit VIII (PsaI), responsible for the structural organization of PsaL required for trimerization (Chitnis & Chitnis, 1993), and BSR22_01362 encoding subunit XII known as PsaM, part of the PSI complex (Schluchter et al., 1996), were both downregulated at 22°C and 26°C (Figure 4), but not at 24°C. The gene encoding the photosystem I assembly protein Ycf4 (BSR22_00088, Figure 4) was upregulated only at 24°C. One gene (BSR22_01930), which encoded a photosystem II reaction centre N protein involved in repairing the PSII reaction centres during

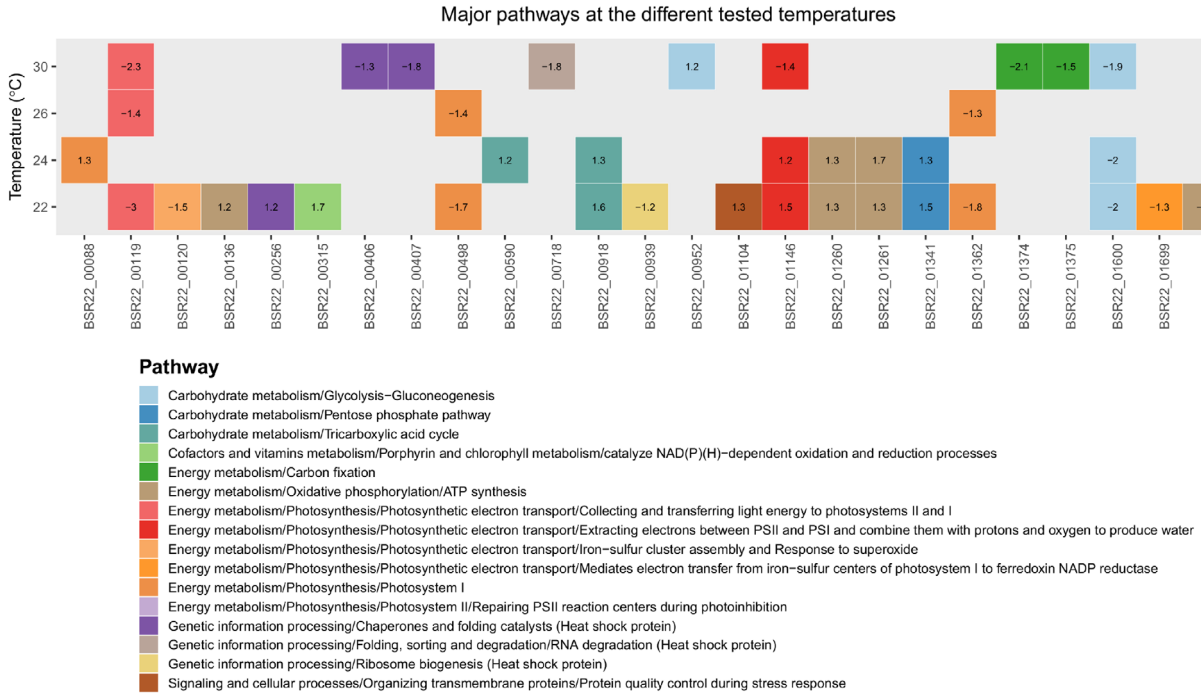

FIGURE 4 Main genes of *Prochlorococcus* RSP50 involved in different pathways that were significantly downregulated (negative values) and upregulated (positive values) at the different temperatures tested, relative to the values found at 28°C. Numbers represents the $\log_2$ fold change of each gene and different pathways are represented by different colours.

photoinhibition (Torabi et al., 2014), was shared between 22°C, 24°C and 30°C, and upregulated with $\log_2$ fold change values that ranged from 1.2 to 1.8 (Figure 4). The general trend for the gene expression profiles of PSI and PSII in *Prochlorococcus* across the different temperatures tested suggests that photosynthesis was detrimentally affected at non-optimal temperatures.

Carbohydrate metabolism in *Prochlorococcus* via the glycolysis pathway was also observed to be detrimentally affected at non-optimal temperatures, particularly at 22°C, 24°C and 30°C. The glyceraldehyde-3-phosphate dehydrogenase-erythrose-4-phosphate dehydrogenase (BSR22_01600) involved in glycolysis was highly downregulated with a mean − 2 $\log_2$ fold change at 22°C, 24°C and 30°C (Figure 4). Instead, the pentose phosphate pathway, which is an alternative to the glycolysis pathway, had the gene BSR22_01341 encoding a transaldolase upregulated at 22°C and 24°C (Figure 4). It is possible that RSP50 relied on the pentose phosphate pathway as an alternative when glycolysis was inhibited at 22°C and 24°C, and hence did not affect the production of acetyl-CoA that entered the tricarboxylic acid (TCA) cycle. This is inferred from the subsequent observation that showed genes linked to TCA cycle, specifically the BSR22_00918 gene encoding the citrate synthase, which was upregulated at 22°C and 24°C (Figure 4), while the BSR22_00590 gene encoding the isocitrate dehydrogenase NADP was found downregulated only at 24°C (Figure 4). The genes (BSR22_01260 and BSR22_01261) encoding the cytochrome c oxidase subunits I and 2, respectively, showed very similar induction responses at 22°C and 24°C (Figure 4). Another gene (BSR22_01146) involved in extracting electrons between PSII and PSI and combining them with protons and oxygen to produce water, was also upregulated at 22°C and 24°C but downregulated at 30°C. In addition, two genes (BSR22_01374 and BSR22_01375) related to carbon fixation and annotated as the carboxysome shell proteins CsoS2 and CsoS3 were highly downregulated at 30°C (Figure 4). These observations suggest that 26°C had no significant detrimental impact on *Prochlorococcus* carbohydrate metabolism compared to 28°C, and that the cyanobacteria was able to rely on alternative carbohydrate metabolic pathways to sustain growth at 22°C and 24°C. However, 30°C showed up as a temperature at which its energy metabolism was relatively more stressed than at the other temperatures.

Heat shock proteins

Heat shock protein genes were downregulated, not upregulated as might be expected, at the highest temperature tested. Thus, the BSR22_00407 gene encoding the 10 kDa chaperonin, the BSR22_00718 gene encoding the chaperone protein DnaK, and the BSR22_00406 gene encoding the 60 kDa chaperonin 2 were highly suppressed at 30°C (Figure 4). However,

in parallel to the downregulation of one heat shock protein at the lowest temperature tested, two other related genes were upregulated. Thus, the BSR22_00939 gene encoding endoribonuclease YbeY (Rasouly et al., 2009) was downregulated by a -1.2 $\log_2$ fold change while the BSR22_00256 gene encoding ATP-dependent Clp protease (Yoo et al., 1996) was upregulated with 1.2 $\log_2$ fold change at 22°C. Another gene (BSR22_01104) annotated as a PDZ domain protein, which is involved in organizing transmembrane proteins was also upregulated by 1.3 $\log_2$ fold change at 22°C (Figure 4).

DISCUSSION

Temperature effects on *Prochlorococcus* growth and primary production.

After 2 months of acclimation at the selected temperatures, the Red Sea *Prochlorococcus* RSP50 surprisingly showed clear evidence of metabolic stress at the warmest value tested, only 2°C higher than the optimal temperature, and experienced at least for 5–6 months per year (Berumen et al., 2019; Raitsos et al., 2011; Raitsos et al., 2013) by natural populations of the HLII ecotype in the area of isolation (Shibl et al., 2016). The specific growth rate of *Prochlorococcus* RSP50 increased significantly with warming from 22°C to 28°C but showed a 11% decrease at 30°C (Figure 1A). The overall 19%–35% lower growth rates observed from changes in chlorophyll *a* rather than in cell abundance could be partly due to the fact that one of the three data points used for calculating chlorophyll *a*-based growth (Figure 1B) was obtained when the cultures were already entering their stationary phase at all temperatures (Figure S1).

Originally formulated for ectotherms (Forster & Hirst, 2012), the temperature size rule (TSR) states that the individual sizes of organisms are expected to become smaller as the temperature increases (Atkinson & Sibly, 1997; Savage et al., 2004), exactly the opposite to our results (Figure 2). A closer examination of Figure 2 shows two effective size clusters, ca. 0.04 μm^3 for the 22–26°C range and ca. 0.06 μm^3 for the two warmest experimental temperatures, although cell size increased systematically from 28°C to 30°C. A positive correlation between cell size and experimental temperature had also been noticed in a *Synechococcus* strain originally isolated from the Red Sea, as well as between environmental temperature and the cell size of a natural *Synechococcus* group in Red Sea shallow waters (Labban et al., 2021). We currently lack an explanation to this unexpected result, which nevertheless cannot be easily explained by diel changes in cell size (Palacio et al., 2020) since our pervasive relationship was based on simultaneous samplings of the five temperature cultures synchronized to the same light–dark cycle. One potential explanation is that the increase in cell size is a way to cope with the warmest temperatures naturally found in tropical regions by accumulating osmolytes, which have been shown to promote thermotolerance in other species such as the anemone *Aiptasia* (Gegner et al., 2017). RSP50 is able to synthesize the osmolyte glucosylglycerol (Shibl et al., 2018), but we did not find any differential expression of the three genes related to glucosylglycerol synthesis (glucosylglycerol-phosphate synthase, glycerol dehydrogenase, and trehalose synthase, Shibl et al., 2018) at the highest temperatures (Table S1).

The C:Chl *a* ratio is an important indication of the physiological status of individual phytoplankton species. Changes in their relative cellular content may be caused by an adjustment of cellular pigment levels to fit photosynthetic demands, for instance light conditions or other abiotic factors (Geider, 1987), by changes in cellular carbon content or a combination of the two (MacIntyre et al., 2002; Calvo-Díaz et al., 2008). The C:Chl *a* ratio is affected by temperature (Geider, 1987) and linked to nutrients availability (Thompson et al., 1992). Under nutrient sufficiency, the C:Chl *a* ratio typically decreases with an increase in temperature, while nutrient deficiency inverts this response (Geider, 1987). *Prochlorococcus* RSP50 did not meet these expectations in a nutrient-replete medium. Rather, our results indicate that the C:Chl *a* ratio in RSP50 was notably lower than current estimates of phytoplankton elsewhere (Guo et al., 2021; Sathyendranath et al., 2009), likely because under nutrient-sufficiency our cyanobacteria had to synthesize relatively more chlorophyll *a* than natural populations in order to capture light (irradiance provided in the incubators was notably lower than ambient levels) in a heavily packed environment with orders of magnitude higher cell concentrations relative to natural conditions (Flombaum et al., 2020). Since C:Chl *a* values were rather invariable up to 28°C and only increased at 30°C, our results suggest that at the optimum temperature the cyanobacteria were able to synthesize more chlorophyll *a* simultaneously to increasing their biovolume, but they failed to do so at 30°C (Figure S3). In the balance between carbon fixation and growth, carbon accumulated relatively to Chl *a* in the warmest temperature culture likely because processes such as cell division were inhibited by thermal stress.

As there was no any added organic carbon source to Pro99 media (Moore et al., 2007), all of the organic carbon observed was ultimately generated photosynthetically by RSP50 in this non-axenic culture. From the perspective of the heterotrophic bacteria present in the culture, DOC produced by RSP50 can follow two pathways: it can be either incorporated into heterotrophic bacterial biomass, or remineralized via bacterial respiration. Given the relatively constant and very high

carrying capacity of *Prochlorococcus* (ca. 300 million cells per ml), it overwhelmingly dominated the bacterial community in the culture (86 ± 13% of total bacterial abundance on average). Although considering biomass rather than abundance, the autotrophic contribution to total bacterial stocks was even higher (1065–1505 vs. 78–228 mg C L^{-1} of heterotrophs, equivalent to 87%–94%), a non-negligible part of the DOC being produced well in excess in the RSP50 cultures was simultaneously processed by heterotrophic bacteria. We included an estimate of that DOC when converting measured BHP values into total carbon requirements or bacterial carbon demand (BCD) using a BGE of 30% (del Giorgio & Cole 1998), which seemed realistic in the nutrient-replete conditions of the cyanobacterial culture (Bertilsson et al., 2005; Obernosterer & Herndl, 1995). As mentioned, these gross dissolved primary production (DPP) estimates were typically double than the measured net DPP values (Table 2). Expectedly, both DPP values increased with temperature similarly to the accumulation of *Prochlorococcus* biomass or particulate primary production (PPP), but the temperature dependence of the sum (i.e. total primary production, TPP = PPP + gross DPP) was extraordinarily strong, explaining 97% of its variance. It was therefore clear that at 30°C more primary production was released extracellularly (i.e. higher PER, Table 2) rather than kept for building up cyanobacteria biomass, which we believe is a consequence of the stressful conditions faced at the warmest temperature (Thornton, 2014).

FDOM is a subset of the CDOM pool that is able to fluoresce, and it is often used as a proxy to trace DOM changes, sources and sinks, both in the natural environment (e.g. Catalá et al., 2016; Coble, 2007; Lønborg & Alvareg-Salgado, 2014; Nieto-Cid et al., 2005; Yamashita & Tanoue, 2008), and in laboratory cultures (e.g. Zhao et al., 2017; Zheng et al., 2019). Two of the distinct FDOM components identified in the incubations (C1 and C3) showed fluorescence properties that are similar to humic-like substances, displaying broad band peaks emitting at wavelengths higher than 400 nm, and similar to Coble peaks M and C, respectively (Coble, 2007; Coble et al., 1998). Component C1 (peak M) was more aliphatic (blue-shifted) than component C3 (peak C). Components C2 and C4, showed narrower spectra, with excitation and emission maxima below 350 nm, and were considered as protein-like substances. C2 was similar to the fluorescent amino acid tyrosine (Coble peak B) while C4 was similar to the fluorescent amino acid tryptophane (Coble peak T) (Coble, 2007; Coble et al., 1998; Yamashita & Tanoue, 2008). The fluorescent components found in the *Prochlorococcus* growing cultures of this study (particularly C1/peak M-, C3/peak C- and C4/peak T-) are consistent with previously reported FDOM components derived from cultured cyanobacteria (Xiao et al., 2021; Zhao et al., 2017) and other phytoplanktonic organisms (Romera-Castillo et al., 2011). Peaks with the same characteristics have been also reported to be widely distributed in the oligotrophic ocean. Catalá and coworkers (Catalá et al., 2016) found peaks C2, C4, C1 and C3, corresponding to C1, C2, C3 and C4 of this study. The reader should keep in mind that the presence of heterotrophic bacteria that grew in our non-axenic cultures (Figure S2) were potentially affecting DOC concentrations and FDOM properties during the incubations. Dissolved free amino acids are regarded as highly labile dissolved products of phytoplankton exudation that can be rapidly consumed by heterotrophic bacteria (Yamashita & Tanoue, 2003, Nieto-Cid 2005). The fluorescent dissolved proteinaceous material (PROT, summatory of fluorescence emitted by tyrosine-like and tryptophane-like amino acid peaks) represents the labile DOC fraction present in the incubations, while the fluorescent humic material (HUM) is considered the refractory DOC pool (Nieto-Cid 2005). In our study there was an increase with temperature treatment of both gross and net DPP (Table 2), while the PROT/HUM ratio decreased (Figure S4B), revealing the likely consumption of labile proteinaceous material during heterotrophic bacterial growth and the accumulation of refractory humic material. This occurred in all cultures and increased with temperature treatment (Figure S2), except at 22°C where the PROT/HUM ratio slightly increased (Figure S4B), likely due to the accumulation of labile proteinaceous DOC when bacterial production rates were lowest (Table 2).

Gene expression in response to temperature

We did not find consistent responses of gene upregulation or downregulation with temperature over the tested range (Figure 4). One possible hypothesis is that protein reactions would run faster at higher temperatures and slower at lower temperatures. Thus, the RSP50 gene expression of these important pathways might appear decreased at higher temperatures while still maintaining elevated protein reaction rates.

The photosynthetic machinery found in cyanobacterial thylakoid membranes is extremely sensitive to heat, with photosystem II (PSII) being the most sensitive part (Mamedov et al., 1993). *Synechocystis* sp. PCC6803 cultures showed an increase in PSII thermotolerance only when grown at higher temperatures (Rowland et al., 2010). During the photosynthetic process, PSII catalyses the water-splitting and oxygen-creation process, whereas the photosystem I (PSI) produces the reducing power for the reduction of $NADP^+$ to NADPH (Gao et al., 2018; Nelson & Yocum, 2006).

The downregulation of most of the genes involved in PSI or responsible for the photosynthetic electron transport in RSP50 at 22°C (Figure 4) implies that NADPH generation was constrained, which might lead to limited photosynthesis at the coolest temperature. Marine *Synechococcus* escape the potentially consequences of low PSI by enrolling into electron transport pathways that are upstream of PSI such as the plastoquinol terminal oxidase (PTOX) (Bailey et al., 2008). Likewise in *Prochlorococcus*, the gene encoding PTOX (BSR22_01146), capable of extracting electrons between PSII and PSI and combining them with protons and oxygen to produce water (Bailey et al., 2008), was also upregulated at 22°C and 24°C but downregulated at the warmest temperature of 30°C (Figure 4). PTOX in plants operates as an alternate electron sink, accounting for up to 30% of total PSII electron flux in response to salt stress (Stepien & Johnson, 2009) and cold temperature (Savitch et al., 2010), suggesting that the upregulation of this gene at 22°C and 24°C in the RSP50 strain was a response to help overcome stress at low temperatures.

Temperature affects the physicochemical availability of CO_2 to cells, as well as their metabolic activities (Paliwal et al., 2017). The downregulation of genes involved in CO_2 fixation in RSP50 acclimated at 30°C (Figure 4) suggests a cellular homeostasis or energy saving mechanism response to stressful conditions at warm temperatures. In contrast, transaldolase, an important enzyme in the pentose phosphate pathway's non-oxidative branch (Sprenger, 1995), was found upregulated only at 22°C and 24°C (Figure 4). In photosynthesizing cells, only the anabolic variant of the non-oxidative pentose phosphate pathway was found to be linked to promoting the photosynthesis direction by substituting the transaldolase step of the catabolic non-oxidative pentose phosphate pathway with a second aldolase reaction and sedoheptulose-1,-7-bisphosphatase (Sharkey, 2021). However, CO_2 was fixed by the transaldolase variant of the Calvin–Benson–Bassham (CBB) cycle, which assimilates CO_2 for the primary production of organic matter, in a chemolithoautotrophic bacterium (Frolov et al., 2019). Transaldolases were also found in two different *Prochlorococcus* strains (MED4 and MIT9313) to be involved in carbon metabolism via reorganizing the carbon skeletons in the pentose phosphate pathway (Tolonen et al., 2006). In addition, citrate synthase, an enzyme required to initiate the oxidative TCA cycle, the most important central carbon pathway and regulator of intracellular ATP production (Tang et al., 2011), was also upregulated at the two lowest temperatures tested (Figure 4). The upregulation of the genes involved in these pathways indicates that RSP50 was still able to efficiently perform essential cellular respiration and carbon fixation at the lowest temperatures (22 and 24°C) but not at 30°C.

Heat shock protein genes

The endoribonuclease YbeY was found to be involved in the processing of 16S, 23S and 5S rRNAs (Davies et al., 2010). In *Escherichia coli*, YbeY is identified as one of the heat shock genes that is necessary for keeping growth at high temperatures and enhancing survival at fatal temperatures (Rasouly et al., 2009), which would agree with the observation of its downregulation in *Prochlorococcus* RSP50 at a temperature well below the thermal stress (Figure 1). Surprisingly, one gene (BSR22_01104) annotated as a PDZ domain protein, which is involved in organizing transmembrane proteins and plays a role in controlling protein quality during stress responses (Muley et al., 2019), was found upregulated only at 22°C (Figure 4). Also, the gene encoding the ATP-dependent Clp protease that potentially acts as a heat shock protein (Yoo et al., 1996) was upregulated at the lowest temperature tested. It is surprising that 2 heat shock proteins were upregulated in RSP50 cells acclimated at 22°C, although growth was impaired at this temperature relative to 28°C, perhaps suggesting that it was still a response to a stressful condition. Although the heat-shock response requires the induction of several proteins collectively known as heat-shock proteins in response to temperature changes (Maleki et al., 2016; Rajaram et al., 2014), the downregulation of three different genes sharing the same functional capacity (10 kDa, DnaK and 60 kDa chaperones) could also indicate that RSP50 acclimated at 30°C might be unable to adapt efficiently to this extreme stress (Figure 4).

CONCLUSIONS

This study sheds light on the potential effect of the expected future warming on HL II *Prochlorococcus*, key primary producers in the surface waters of the Red Sea (Al-Otaibi et al., 2020; Coello-Camba et al., 2020) and in the vast tropical and subtropical regions of the world ocean (Agusti et al., 2019; Flombaum et al., 2013). Increasing temperature resulted in higher specific growth rates, reaching their maximum at 28°C, and larger cell sizes, which was especially marked at 30°C. Global transcriptomic analysis showed that the strain RSP50 responded differently to temperature within the natural range of the Red Sea. Lower temperatures had a greater impact on the gene expression of the strain RSP50 than higher temperatures, as shown by the higher temperature-responsive gene numbers, which suggests the RSP50 cells may finely tune their metabolic pathways to grow at lower temperatures (up to 6°C cooler than the optimal) but they might not be able to cope effectively at the highest temperature tested. In particular, RSP50 repressed genes involved in key metabolic pathways, including carbon fixation and

photosynthetic electron transport, at 30°C. These findings, together with an increase in the relative amount of photosynthate being released extracellularly, collectively indicate that RSP50 already experienced stressful conditions at 30°C. Temperatures warmer than 28°C, not unusual in many parts of the Red Sea in summer (Berumen et al., 2019; Raitsos et al., 2013; Rasul et al., 2015), could effectively be detrimental to *Prochlorococcus* RSP50. We conclude that Red Sea *Prochlorococcus* populations, currently subject to the highest natural seawater temperatures on earth, may have difficulties to adapt to future global warming.

EXPERIMENTAL PROCEDURES

Culture conditions and sampling

The original *Prochlorococcus* RSP50 (Shibl et al., 2018) non-axenic culture was maintained in artificial based Pro99 medium with ~38 of salinity at 27°C (the mean temperature of the isolation area) under 115 μmol photons m^{-2} s^{-1} irradiance in a 12:12 h light: dark cycle until the start of the temperature acclimation and subsequent experiments.

Four true replicates of non-axenic RSP50 cultures grown at 27°C, with an initial concentration of 10^5 cells ml^{-1}, were gradually acclimated at five temperatures (22°C, 24°C, 26°C, 28°C and 30°C) at 1–2°C steps (increase or decrease). Although this procedure was taken in order to avoid lethal thermal stress, *Prochlorococcus* cells did not survive at temperatures higher than 30°C. Cyanobacteria samples were collected daily during the light cycle at the same time and preserved in glutaraldehyde (final concentration of 0.025%), then incubated in the dark for 10 min and stored at −80°C to be analysed by flow cytometry (Palacio et al., 2020). Samples for heterotrophic bacteria were concurrently collected for each replicate and temperature at the initial (day 0) and final time (after 8, 9 and 11 days of incubation at 30–28–26°C, 24°C and 22°C, respectively), as well as during the logarithmic growth phase [after 6, 7 and 9 days of incubation at 30–28–26°C, 24°C and 22°C, respectively (Figure S2)], where the abundance of *Prochlorococcus* had reached ~7.5×10^7cells ml^{-1} (Figure S1). Samples of each replicate and temperature were also sampled for chlorophyll *a* concentration at the initial (day 0) and final time (after 8, 9 and 11 days of incubation at 30–28–26°C, 24°C and 22°C, respectively), and additionally when the abundance reached around ~7.5×10^7cells ml^{-1}(Figure S1). About 10 to 30 ml were filtered through 0.2 μm polycarbonate filters and then stored at −80°C until analysis. Pigments were extracted in 90% acetone for 24 h in the dark at 4°C and chlorophyll *a* was measured using a Turner model Trilogy fluorometer calibrated with known concentrations of pure chlorophyll *a*. We additionally sampled for inorganic nutrients, dissolved organic matter and RNA at the same time of collection of the flow cytometry samples, although the frequency of sampling differed as detailed below.

Flow cytometry

Cell abundance was measured using a BD FACSCanto II flow cytometer. The samples were stored, stained, and analysed following Labban et al. (2021). The cytograms were analysed with the BD Paint-A-Gate software, which allowed us to clearly separate *Prochlorococcus* RSP50 cells from heterotrophic bacteria based on the red fluorescence (PerCP-Cy5-5, 498 nm) versus right angle light or side scatter (SSC) signals, as well as red versus orange fluorescence (PE, 433 nm) signals. The absolute abundances of *Prochlorococcus* and heterotrophic bacteria were calculated based on the actual flow rate and the time each sample took to reach 10,000 events.

Mean (i.e. average of four replicates) specific growth rates (μ, day^{-1}) of RSP50 were estimated as the slopes of ln-transformed cell abundance versus time for the exponential growth phase (Huete-Stauffer et al., 2015). The Chl *a*-based growth rate (day^{-1}) of *Prochlorococcus* was similarly estimated as the slope of ln-transformed chlorophyll *a* concentration versus time. Bacterial size was calculated as biovolume in μm^3, assuming a spherical shape. Cell diameter (μm) was first estimated using the relationship: $\mu m = 1.62 + 0.87$ log relSSC, with relSSC representing the RSP50 cells SSC values relative to the SSC of 1 μm fluorescent latex beads (Molecular Probes, ref. F-13081) (Calvo-Díaz & Morán, 2006). Biovolume was converted into cellular carbon content (CCC) using 240 fgC μm^{-3} for *Prochlorococcus* (Worden et al., 2004) and the allometric relationship fgC $cell^{-1} = 108.8 \times (\text{biovolume})^{0.898}$ for the associated heterotrophic bacteria (Gundersen et al., 2002). *Prochlorococcus* RSP50 and heterotrophic bacteria biomass was finally obtained by multiplying CCC by their corresponding abundances.

Chromophoric and fluorescent dissolved organic matter, dissolved organic carbon, and inorganic nutrients

To estimate total primary production of *Prochlorococcus* RSP50 cultures, replicates at each temperature (22°C, 24°C, 26°C, 28°C and 30°C) were sampled at the initial (day 0) and final time (after 8, 9 and 11 days of incubation at 30–28–26°C, 24°C and 22°C respectively), as well as during the logarithmic growth phase (after 6, 7 and 9 days of incubation at 30–28–26°C, 24°C and 22°C, respectively) where the abundance

reached around $\sim 7.5 \times 10^7$ cells ml^{-1} (Figure S1). The samples were then filtered through 0.2 μm polycarbonate filters. Forty millilitres of filtered samples were acidified with H_3PO_4 to a pH = 1–2, stored at 4°C, and analysed by high temperature catalytic oxidation (HTCO) using a Shimadzu TOC-L analyser (Sharp et al., 2002) to measure the dissolved organic carbon (DOC).

Additionally, 10 ml of filtered samples were analysed using a Horiba Jobin Yvon AquaLog spectrofluorometer (Wünsch et al., 2015) to determine the chromophoric (absorbance spectra) and fluorescent (excitation emission matrices) dissolved organic matter (DOM) [i.e. Chromophoric and fluorescent dissolved organic matter (CDOM and FDOM), respectively]. A total of 62 three-dimensional fluorescence excitation emission matrices (EEMs) were recorded by scanning between 240 and 600 nm (excitation) and 250–600 nm (emission), at 3 nm increments. To correct and calibrate the fluorescence spectra post-processing steps were followed according to (Murphy et al., 2010), in which Raman-normalized Milli-Q blanks were subtracted to remove the Raman scattering signal (Stedmon et al., 2003). All fluorescence spectra were Raman area (RA) normalized by the subtraction of daily blanks performed using Ultra-Pure Milli-Q sealed water (Certified Reference, Starna Cells). Inner-filter correction (IFC) was also applied according to (McKnight et al., 2001). MATLAB (version R2018b) was used for the RA normalization, blank subtraction, IFC and generation of EEMs. The EEMs obtained were subjected to PARAFAC modelling using drEEM Toolbox (Murphy et al., 2013) and the model was validated using half split validation and random initialization (Stedmon & Bro, 2008).

Finally, 15 ml were stored frozen at −20°C for inorganic nutrient analysis. Nitrate (NO_3^-), nitrite (NO_2^-) and phosphate (PO_4^{3-}) were analysed by colorimetry using a Bruan and Luebbe Autoanalyser (Hansen & Koroleff, 1999).

Total RNA extraction and sequencing

Forty millilitres of each replicate at each temperature was collected when *Prochlorococcus* reached the exponential phase ($\sim 7.5 \times 10^7$ cells ml^{-1}) (Figure S1) and centrifuged at 16,084.8×g for 10 min at 4°C. One millilitre of RNAprotect (Qiagen, Valencia, CA) was added to the concentrated culture then stored at −80°C for up to 4 weeks. Total RNA was extracted using the RNeasy Mini kit (Qiagen, Hilden, Germany) with the on-column DNase treatment. RNA quality was determined using an Agilent 2200 bioanalyzer (Agilent Technologies, Santa Clara, CA). Samples were then submitted for RNA-seq on the Illumina HiSeq platform in the KAUST Genomics Core Lab facility. Before sequencing, the RiboZero rRNA removal kit (Illumina, San Diego, CA, USA) was used to remove bacterial ribosomal RNA from 1 μg of total RNA. Following the manufacturer's protocols, the enriched mRNA fraction was converted to RNA-seq libraries compatible for runs on Illumina HiSeq platforms. Raw fastq files were then generated by the KAUST Bioinformatics Core Lab.

RNA-seq data analysis

Raw RNA-sequencing reads were quality trimmed using Trimmomatic v0.36 (Bolger et al., 2014), with a minimum length of 75 bp. Quality trimmed reads were then mapped to the RSP50 genome (NCBI accession #CP018344) with Bowtie2 v2.4.1 (Langmead & Salzberg, 2012) and the generated files were processed with SAMtools v1.5 (Li et al., 2009). The tool featureCounts (Liao et al., 2014) was used to obtain read counts per gene and differentially expressed genes (DEGs) were identified using DESeq2 v1.14.1 (Love et al., 2014) at a false discovery rate (FDR) of *p*-adjusted value <0.05 and a minimum $\log_2$ fold change of 1.2. Transcriptomic data at 28°C was used as a control for the differential expressions analysis at all other tested temperatures.

We classified these differentially expressed genes into functional groups using KEGG pathway database to determine their functions. Other than genes of uncharacterized proteins, differentially expressed genes involved in energy metabolism, including photosynthesis, oxidative phosphorylation, and cellular carbon fixation and respiration, were the highest number of genes and most of them were highly upregulated or downregulated (Table S1). Using a temperature-dependent response to the gene expression and high number upregulated or downregulated genes criteria, the transcriptomic assessments will also include genes involved in heat shock proteins.

AUTHOR CONTRIBUTIONS

Abbrar Labban: Investigation (equal); methodology (equal); visualization (equal); writing – original draft (equal); writing – review and editing (equal). **Ahmed A. Shibl:** Investigation (equal); methodology (equal); visualization (equal); writing – review and editing (equal). **Maria Ll. Calleja:** Investigation (equal); methodology (equal); visualization (equal); writing – review and editing (equal). **Peiying Hong:** Conceptualization (equal); investigation (equal); supervision (equal); writing – review and editing (equal). **Xosé Anxelu G. Morán:** Conceptualization (equal); investigation (equal); writing-review and editing (equal); supervision (equal); funding acquisition(equal); project administration (equal).

ACKNOWLEDGEMENTS

This work was supported by King Abdullah University of Science and Technology (KAUST) baseline to Xosé

Anxelu G. Morán. The authors acknowledge Miguel Viegas for analysing chlorophyll *a* data. The authors thank Eman Sabbagh, Ghaida Hadaidi, Saeed Amin, and Najwa Al-Otaibi for their assistance with sample filtration. The authors would like also to thank KAUST Bioscience Core Lab (BCL) for sequencing.

CONFLICT OF INTEREST

The authors have no conflicts of interest to declare and declare that all of the reported work is original.

DATA AVAILABILITY STATEMENT

The sequences data were deposited in NCBI-Bio Project PRJNA755949.

ORCID

Abbrar Labban https://orcid.org/0000-0002-7415-6361
Ahmed A. Shibl https://orcid.org/0000-0002-8147-8406
Maria Ll. Calleja https://orcid.org/0000-0002-5992-2013
Pei-Ying Hong https://orcid.org/0000-0002-4474-6600
Xosé Anxelu G. Morán https://orcid.org/0000-0002-9823-5339

REFERENCES

Agusti, S., Lubián, L.M., Moreno-Ostos, E., Estrada, M. & Duarte, C. M. (2019) Projected changes in photosynthetic picoplankton in a warmer subtropical ocean. *Frontiers in Marine Science*, 506.

Al-Otaibi, N., Huete-Stauffer, T.M., Calleja, M.L., Irigoien, X. & Moran, X.A.G. (2020) Seasonal variability and vertical distribution of autotrophic and heterotrophic picoplankton in the Central Red Sea. *PeerJ*, 8, e8612.

Atkinson, D. & Sibly, R.M. (1997) Why are organisms usually bigger in colder environments? Making sense of a life history puzzle. *Trends in Ecology & Evolution*, 12, 235–239.

Bailey, S., Melis, A., Mackey, K.R., Cardol, P., Finazzi, G., van Dijken, G. et al. (2008) Alternative photosynthetic electron flow to oxygen in marine Synechococcus. *Biochimica et Biophysica Acta*, 1777(3), 269–276.

Bertilsson, S., Berglund, O., Pullin, M.J. & Chisholm, S.W. (2005) Release of dissolved organic matter by Prochlorococcus. *Vie et Milieu*, 55, 225–232.

Berumen, M.L., Voolstra, C.R., Daffonchio, D., Agusti, S., Aranda, M., Irigoien, X. et al. (2019) The Red Sea: environmental gradients shape a natural laboratory in a nascent ocean. In: Voolstra, C. R. & M.L. (Eds.) *Coral reefs of the Red Sea*. Cham: Springer International Publishing, pp.1–10.

Biller, S.J., Berube, P.M., Lindell, D. & Chisholm, S.W. (2015) Prochlorococcus: the structure and function of collective diversity. *Nature Reviews. Microbiology*, 13(1), 13–27.

Bolger, A.M., Lohse, M. & Usadel, B. (2014) Trimmomatic: a flexible trimmer for Illumina sequence data. *Bioinformatics*, 30(15), 2114–2120.

Bouman, H.A., Ulloa, O., Scanlan, D.J., Zwirglmaier, K., Li, W.K., Platt, T. et al. (2006) Oceanographic basis of the global surface distribution of Prochlorococcus ecotypes. *Science*, 312(5775), 918–921.

Calvo-Díaz, A. & Morán, X.A.G. (2006) Seasonal dynamics of picoplankton in shelf waters of the southern Bay of Biscay. *Aquatic Microbial Ecology*, 42, 159–174.

Calvo-Díaz, A., Morán, X.A.G. & Suárez, L.Á. (2008) Seasonality of picophytoplankton chlorophyll a and biomass in the central Cantabrian Sea, southern Bay of Biscay. *Journal of Marine Systems*, 72(1–4), 271–281.

Catalá, T.S., Álvarez-Salgado, X.A., Otero, J., Iuculano, F., Companys, B., Horstkotte, B. et al. (2016) Drivers of fluorescent dissolved organic matter in the global epipelagic ocean. *Limnology and Oceanography*, 61(3), 1101–1119.

Chitnis, V.P. & Chitnis, P.R. (1993) PsaL subunit is required for the formation of photosystem I trimers in the cyanobacterium Synechocystis sp. PCC 6803. *FEBS*, 336, 330–334.

Coble, P.G. (2007) Marine optical biogeochemistry: the chemistry of ocean color. *Chemical Reviews*, 107, 402–418.

Coble, P.G., Del Castillo, C.E. & Avril, B. (1998) Distribution and optical properties of CDOM in the Arabian Sea during the 1995 southwest monsoon. *Deep Sea Research. Part II Topical Studies in Oceanography*, 45(10–11), 2195–2223.

Coello-Camba, A., Diaz-Rua, R., Duarte, C.M., Irigoien, X., Pearman, J.K., Alam, I.S. et al. (2020) Picocyanobacteria community and Cyanophage infection responses to nutrient enrichment in a Mesocosms experiment in oligotrophic waters. *Frontiers in Microbiology*, 11, 1153.

Coma, R., Ribes, M., Serrano, E., Jimenez, E., Salat, J. & Pascual, J. (2009) Global warming-enhanced stratification and mass mortality events in the Mediterranean. *Proceedings of the National Academy of Sciences*, 106(15), 6176–6181.

Daufresne, M., Lengfellner, K. & Sommer, U. (2009) Global warming benefits the small in aquatic ecosystems. *Proceedings of the National Academy of Sciences*, 106(31), 12788–12793.

Davies, B.W., Köhrer, C., Jacob, A.I., Simmons, L.A., Zhu, J., Aleman, L.M. et al. (2010) Role of Escherichia coli YbeY, a highly conserved protein, in rRNA processing. *Molecular Microbiology*, 78(2), 506–518.

Doney, S.C., Ruckelshaus, M., Emmett Duffy, J., Barry, J.P., Chan, F., English, C.A. et al. (2012) Climate change impacts on marine ecosystems. *Annual Review of Marine Science*, 4, 11–37.

Flombaum, P., Gallegos, J.L., Gordillo, R.A., Rincón, J., Zabala, L.L., Jiao, N. et al. (2013) Present and future global distributions of the marine cyanobacteria Prochlorococcus and Synechococcus. *Proceedings of the National Academy of Sciences*, 110(24), 9824–9829.

Flombaum, P., Wang, W.-L., Primeau, F.W. & Martiny, A.C. (2020) Global picophytoplankton niche partitioning predicts overall positive response to ocean warming. *Nature Geoscience*, 13(2), 116–120.

Forster, J. & Hirst, A.G. (2012) The temperature-size rule emerges from ontogenetic differences between growth and development rates. *Functional Ecology*, 26, 483–492.

Frolov, E.N., Kublanov, I.V., Toshchakov, S.V., Lunev, E.A., Pimenov, N.V., Bonch-Osmolovskaya, E.A. et al. (2019) Form III RubisCO-mediated transaldolase variant of the Calvin cycle in a chemolithoautotrophic bacterium. *PNAS*, 116, 18638–18646.

Fuller, N.J., West, N.J., Marie, D., Yallop, M., Rivlin, T., Post, A.F. et al. (2005) Dynamics of community structure and phosphate status of picocyanobacterial populations in the Gulf of Aqaba, Red Sea. *Limnology and Oceanography*, 50, 363–375.

Gao, J., Wang, H., Yuan, Q. & Feng, Y. (2018) Structure and function of the photosystem supercomplexes. *Frontiers in Plant Science*, 9, 357.

Gegner, H.M., Ziegler, M., Radecker, N., Buitrago-Lopez, C., Aranda, M. & Voolstra, C.R. (2017) High salinity conveys thermotolerance in the coral model Aiptasia. *Biology Open*, 6(12), 1943–1948.

Geider, R.J. (1987) Light and temperature dependence of the carbon to chlorophyll a ratio in microalgae and cyanobacteria: implications for physiology and growth of phytoplankton. *The New Phytologist*, 106, 1–34.

Geider, R.J., Moore, C.M. & Suggett, D.J. (2014) Ecology of marine phytoplankton. In: Monson, R.K. (Ed.) *Ecology and the environment*. New York: Springer, pp. 483–531.

Gundersen, K., Heldal, M., Norland, S., Purdie, D.A.A. & Knap, A.H. H. (2002) Elemental C, N, and P cell content of individual bacteria collected at the Bermuda Atlantic time-series study (BATS) site. *Limnology and Oceanography*, 47, 1525–1530.

Guo, S., Zhao, Z., Liang, J., Du, J. & Sun, X. (2021) Carbon biomass, carbon-to-chlorophyll a ratio and the growth rate of phytoplankton in Jiaozhou Bay, China. *Journal of Oceanology and Limnology*, 39(4), 1328–1342.

Hansen, H.P. & Koroleff, F. (1999) Determination of nutrients. In: Grasshoff, K., Kremling, K. & Manfred, E. (Eds). *Methods of seawater analysis*. Weinheim: Wiley-VCH, pp. 159–228.

Huete-Stauffer, T.M., Arandia-Gorostidi, N., Diaz-Perez, L. & Moran, X.A.G. (2015) Temperature dependence of growth rates and carrying capacities of marine bacteria depart from metabolic theoretical predictions. *FEMS Microbiology Ecology*, 91, fiv111.

Johnson, Z.I., Zinser, E.R., Coe, A., McNulty, N.P., Woodward, E.M. S. & Chisholm, S.W. (2006) Niche partitioning among Prochlorococcus ecotypes along ocean-scale environmental gradients. *Science*, 311, 1737–1739.

Labban, A., Palacio, A.S., García, F.C., Hadaidi, G., Ansari, M.I., López-Urrutia, Á. et al. (2021) Temperature responses of heterotrophic bacteria in co-culture with a Red Sea Synechococcus strain. *Frontiers in Microbiology*, 12, 612732.

Langmead, B. & Salzberg, S.L. (2012) Fast gapped-read alignment with bowtie 2. *Nature Methods*, 9(4), 357–359.

Li, H., Handsaker, B., Wysoker, A., Fennell, T., Ruan, J., Homer, N. et al. (2009) The sequence alignment/map format and SAMtools. *Bioinformatics*, 25(16), 2078–2079.

Liao, H.L., Chen, Y., Bruns, T.D., Peay, K.G., Taylor, J.W., Branco, S. et al. (2014) Metatranscriptomic analysis of ectomycorrhizal roots reveals genes associated withPiloderma-Pinussymbiosis: improved methodologies for assessing gene expressionin situ. *Environmental Microbiology*, 16(12), 3730–3742.

Lindell, D. & Post, A.F. (1995) Ultraphytoplankton successionis triggered by deep winter mixing in the Gulf of Aqaba (Eilat), Red Sea. *Limnology and Oceanography*, 40, 1130–1141.

Love, M.I., Huber, W. & Anders, S. (2014) Moderated estimation of fold change and dispersion for RNA-seq data with DESeq2. *Genome Biology*, 15(12), 550.

Lønborg, C. & Alvareg-Salgado, X.A. (2014) Tracing dissolved organic matter cycling in the eastern boundary of the temperate North Atlantic using absorption and fluorescence spectroscopy. *Deep-Sea Research Part I: Oceanographic Research Papers*, 85, 35–46.

Ma, L., Calfee, B.C., Morris, J.J., Johnson, Z.I. & Zinser, E.R. (2017) Degradation of hydrogen peroxide at the ocean's surface: the influence of the microbial community on the realized thermal niche of Prochlorococcus. *The ISME Journal*, 12(2), 473–484.

MacIntyre, H.L., Kana, T.M., Anning, T. & Geider, R.J. (2002) Photoacclimation of photosynthesis irradiance response curves and photosynthetic pigments in microalgae and cyanobacteria. *Journal of Phycology*, 38, 17–38.

Maleki, F., Khosravi, A., Nasser, A., Taghinejad, H. & Azizian, M. (2016) Bacterial heat shock protein activity. *Journal of Clinical and Diagnostic Research*, 10(3), BE01-03.

Mamedov, M., Hayashi, H. & Murata, N. (1993) Effects of glycinebetaine and unsaturation of membrane-lipids on heat-stability of photosynthetic electron-transport and phosphorylation reactions in Synechocystis PCC6803. *Biochimica et Biophysica Acta*, 1142, 1–5.

McKnight, D.M., Boyer, E.W., Westerhoff, P.K., Doran, P.T., Kulbe, T. & Andersen, D.T. (2001) Spectrofluorometric characterization of dissolved organic matter for indication of precursor organic material and aromaticity. *Limnology and Oceanography*, 46, 38–48.

Moore, L.R. & Chisholm, S.W. (1999) Photophysiology of the marine cyanobacterium Prochlorococcus: ecotypic differences among cultured isolates. *Limnology and Oceanography*, 44, 628–638.

Moore, L.R., Coe, A., Zinser, E.R., Saito, M.A., Sullivan, M.B., Lindell, D. et al. (2007) Culturing the marine cyanobacterium Prochlorococcus. *Limnology and Oceanography*, 5, 353–362.

Moore, L.R., Goericke, R. & Chisholm, S.W. (1995) Comparative physiology of Synechococcus and Prochlorococcus: influence of light and temperature on growth, pigments, fluorescence and absorptive properties. *Marine Ecology Progress Series*, 116, 259–275.

Moore, L.R., Rocap, G. & Chisholm, S.W. (1998) Physiology and molecular phylogeny of coexisting Prochlorococcus ecotypes. *Nature*, 393, 464–467.

Morel, A., Ahn, Y.-H., Partensky, F., Vaulot, D. & Claustre, H. (1993) Prochlorococcus and Synechococcus: a comparative study of their optical properties in relation to their size and pigmentation. *Journal of Marine Research*, 51, 617–649.

Morris, J.J., Johnson, Z.I., Szul, M.J., Keller, M. & Zinser, E.R. (2011) Dependence of the cyanobacterium Prochlorococcus on hydrogen peroxide scavenging microbes for growth at the ocean's surface. *PLoS One*, 6(2), e16805.

Morris, J.J., Kirkegaard, R., Szul, M.J., Johnson, Z.I. & Zinser, E.R. (2008) Facilitation of robust growth of Prochlorococcus colonies and dilute liquid cultures by "helper" heterotrophic bacteria. *Applied and Environmental Microbiology*, 74(14), 4530–4534.

Muley, V.Y., Akhter, Y., Galande, S. & Gojobori, T. (2019) PDZ domains across the microbial world: molecular link to the proteases, stress response, and protein synthesis. *Genome Biology and Evolution*, 11(3), 644–659.

Murphy, K.R., Butler, K.D., Spencer, R.G.M., Stedmon, C.A., Boehme, J.R. & Aiken, G.R. (2010) Measurement of dissolved organic matter fluorescence in aquatic environments: an interlaboratory comparison. *Environmental Science & Technology*, 44, 9405–9412.

Murphy, K.R., Stedmon, C.A., Graeber, D. & Bro, R. (2013) Fluorescence spectroscopy and multi-way techniques. PARAFAC. *Analytical Methods*, 5(23), 6557.

Needoba, J.A., Foster, R.A., Sakamto, C., Zehr, J.P. & Johnson, K.S. (2007) Nitrogen fixation by unicellular diazotrophic cyanobacteria in the temperate oligotrophic North Pacific Ocean. *Limnology and Oceanography*, 52, 1317–1327.

Nelson, N. & Yocum, C.F. (2006) Structure and function of photosystems I and ii. *Annual Review of Plant Biology*, 57(1), 521–565.

Ngugi, D.K., Antunes, A., Brune, A. & Stingl, U. (2012) Biogeography of pelagic bacterioplankton across an antagonistic temperature-salinity gradient in the Red Sea. *Molecular Ecology*, 21(2), 388–405.

Nieto-Cid, M., Alvarez-Salgado, X.A., Gago, J. & Pérez, F.F. (2005) DOM fluorescence, a tracer for biogeochemical processes in a coastal upwelling system (NW Iberian Peninsula). *Marine Ecololgy Progress Series*, 297, 33–50.

Obernosterer, I. & Herndl, G.J. (1995) Phytoplankton extracellular release and bacterial growth: dependence on the inorganic N: P ratio. *Marine Ecology Progress Series*, 116, 247–257.

Palacio, A.S., Cabello, A.M., García, F.C., Labban, A., Morán, X.A.G., Garczarek, L. et al. (2020) Changes in population age-structure obscure the temperature-size rule in marine cyanobacteria. *Frontiers in Microbiology*, 11, 1–11.

Paliwal, C., Mitra, M., Bhayani, K., Bharadwaj, S.V.V., Ghosh, T., Dubey, S. et al. (2017) Abiotic stresses as tools for metabolites in microalgae. *Bioresource Technology*, 244, 1216–1226.

Partensky, F., Hess, W.R. & Vaulot, D. (1999) Prochlorococcus, a marine photosynthetic prokaryote of global significance. *Microbiology and Molecular Biology Reviews*, 63, 106–127.

Raitsos, D.E., Hoteit, I., Prihartato, P.K., Chronis, T., Triantafyllou, G. & Abualnaja, Y. (2011) Abrupt warming of the Red Sea. *Geophysical Research Letters*, 38(14), L14601.

Raitsos, D.E., Pradhan, Y., Brewin, R.J., Stenchikov, G. & Hoteit, I. (2013) Remote sensing the phytoplankton seasonal succession of the Red Sea. *PLoS One*, 8(6).

Rajaram, H., Chaurasia, A.K. & Apte, S.K. (2014) Cyanobacterial heat-shock response: role and regulation of molecular chaperones. *Microbiology*, 160, 647–658.

Rasouly, A., Schonbrun, M., Shenhar, Y. & Ron, E.Z. (2009) YbeY, a heat shock protein involved in translation in Escherichia coli. *Journal of Bacteriology*, 191(8), 2649–2655.

Rasul, N.M.A., Stewart, I.C.F. & Nawab, Z.A. (2015) *Introduction to the Red Sea: its origin, structure, and environment*. Berlin, Heidelberg: Springer, pp. 1–28.

Raven, J.A. & Geider, R.J. (1988) Temperature and algal growth. *The New Phytologist*, 110, 441–461.

Rocap, G., Distel, D.L., Waterbury, J.B. & Chisholm, S.W. (2002) Resolution of Prochlorococcus and Synechococcus ecotypes by using 16 S-23 S ribosomal DNA internal transcribed spacer sequences. *Applied and Environmental Microbiology*, 68(3), 1180–1191.

Romera-Castillo, C., Sarmento, H., Álvarez-Salgado, X.A., Gasol, J. M. & Marrasé, C. (2011) Net production and consumption of fluorescent colored dissolved organic matter by natural bacterial assemblages growing on marine phytoplankton exudates. *Applied and Environmental Microbiology*, 77(21), 7490–7498.

Rowland, J.G., Pang, X., Suzuki, I., Murata, N., Simon, W.J. & Slabas, A.R. (2010) Identification of components associated with thermal acclimation of photosystem II in Synechocystis sp. PCC6803. *PLoS One*, 5(5), e10511.

Sathyendranath, S., Stuart, V., Nair, A., Oka, K., Nakane, T., Bouman, H. et al. (2009) Carbon-to-chlorophyll ratio and growth rate of phytoplankton in the sea. *Marine Ecology Progress Series*, 383, 73–84.

Savage, V.M., Gillooly, J.F., Brown, J.H., West, G.B. & Charnov, E.L. (2004) Effects of body size and temperature on population growth. *The American Naturalist*, 163, 429–441.

Savitch, L.V., Ivanov, A.G., Krol, M., Sprott, D.P., Öquist, G. & Huner, N.P.A. (2010) Regulation of energy partitioning and alternative electron transport pathways during cold acclimation of Lodgepole pine is oxygen dependent. *Plant and Cell Physiology*, 51(9), 1555–1570.

Scanlan, D.J., Ostrowski, M., Mazard, S., Dufresne, A., Garczarek, L., Hess, W.R. et al. (2009) Ecological genomics of marine picocyanobacteria. *Microbiology and Molecular Biology Reviews*, 73(2), 249–299.

Schluchter, W.M., Shen, G., Zhao, J. & Bryant, D.A. (1996) Characterization of psaI and psaL mutants of Synechococcus sp. strain PCC 7002: a new model for state transitions in cyanobacteria. *Photochemistry and Photobiology*, 64, 53–66.

Sharkey, T.D. (2021) Pentose phosphate pathway reactions in photosynthesizing cells. *Cell*, 10(6),1547.

Sharp, J.H., Carlson, C.A., Peltzer, E.T., Castle-Ward, D.M., Savidge, K.B. & Rinker, K.R. (2002) Final dissolved organic carbon broad community intercalibration and preliminary use of DOC reference materials. *Marine Chemistry*, 77, 239–253.

Shibl, A.A., Haroon, M.F., Ngugi, D.K., Thompson, L.R. & Stingl, U. (2016) Distribution of Prochlorococcus ecotypes in the Red Sea basin based on analyses of rpoC1 sequences. *Frontiers in Marine Science*, 3, 104.

Shibl, A.A., Ngugi, D.K., Talarmin, A., Thompson, L.R., Blom, J. & Stingl, U. (2018) The genome of a novel isolate of *Prochlorococcus* from the Red Sea contains transcribed genes for compatible solute biosynthesis. *FEMS Microbiology Ecology*, 94(12), fiy182.

Shibl, A.A., Thompson, L.R., Ngugi, D.K. & Stingl, U. (2014) Distribution and diversity of Prochlorococcus ecotypes in the Red Sea. *FEMS Microbiology Letters*, 356(1), 118–126.

Sofianos, S.S. & Johns, W.E. (2007) Observations of the summer Red Sea circulation. *Journal of Geophysical Research*, 112, C06025.

Sprenger, G.A. (1995) Genetics of pentose-phosphate pathway enzymes of Escherichia coli K-12. *Archives of Microbiology*, 164, 324–330.

Stedmon, C.A. & Bro, R. (2008) Characterizing dissolved organic matter fluorescence with parallel factor analysis: a tutorial. *Limnology and Oceanography: Methods*, 6(11), 572–579.

Stedmon, C.A., Markager, S. & Bro, R. (2003) Tracing dissolved organic matter in aquatic environments using a new approach to fluorescence spectroscopy. *Marine Chemistry*, 82(3–4), 239–254.

Stepien, P. & Johnson, G.N. (2009) Contrasting responses of photosynthesis to salt stress in the Glycophyte Arabidopsis and the halophyte Thellungiella: role of the plastid terminal oxidase as an alternative electron sink. *Plant Physiology*, 149(2), 1154–1165.

Tang, K.H., Tang, Y.J. & Blankenship, R.E. (2011) Carbon metabolic pathways in phototrophic bacteria and their broader evolutionary implications. *Frontiers in Microbiology*, 2, 165.

Thompson, P.A., Guo, M.X. & Harrison, P.J. (1992) Effects of variation in temperature. I. On the biochemical composition of 8 species of marine phytoplankton. *Journal of Phycology*, 28, 481–488.

Thornton, D.C.O. (2014) Dissolved organic matter (DOM) release by phytoplankton in the contemporary and future ocean. *European Journal of Phycology*, 49(1), 20–46.

Ting, C.S., Rocap, G., King, J. & Chisholm, S.W. (2002) Cyanobacterial photosynthesis in the oceans: the origins and significance of divergent light-harvesting strategies. *Trends in Microbiology*, 10, 134–142.

Tolonen, A., Aach, J., Lindell, D., Johnson, Z.I., Rector, T., Steen, R. et al. (2006) Global gene expression of Prochlorococcus ecotypes in response to changes in nitrogen availability. *Molecular Systems Biology*, 2, 53.

Torabi, S., Umate, P., Manavski, N., Plöchinger, M., Kleinknecht, L., Bogireddi, H. et al. (2014) PsbN is required for assembly of the photosystem II reaction center in Nicotiana tabacum. *The Plant Cell*, 26(3), 1183–1199.

West, N.J. & Scanlan, D.J. (1999) Niche-partitioning of Prochlorococcus populations in a stratified water column in the eastern North Atlantic Ocean. *Applied and Environmental Microbiology*, 65, 2585–2591.

Worden, A.Z., Nolan, J.K. & Palenik, B. (2004) Assessing the dynamics and ecology of marine picophytoplankton: the importance of the eukaryotic component. *Limnology and Oceanography*, 49, 168–179.

Wünsch, U.J., Murphy, K.R. & Stedmon, C.A. (2015) Fluorescence quantum yields of natural organic matter and organic compounds: implications for the fluorescence-based interpretation of organic matter composition. *Frontiers in Marine Science*, 2, 98.

Xiao, X., Guo, W., Li, X., Wang, C., Chen, X., Lin, X. et al. (2021) Viral lysis alters the optical properties and biological availability of dissolved organic matter derived from Prochlorococcus picocyanobacteria. *Applied and Environmental Microbiology*, 87(3), e02271-20.

Yamashita, Y. & Tanoue, E. (2003) Chemical characterization of protein-like fluorophores in DOM in relation to aromatic amino acids. *Marine Chemistry*, 82, 255–271.

Yamashita, Y. & Tanoue, E. (2008) Production of bio-refractory fluorescent dissolved organic matter in the ocean interior. *Nature Geoscience*, 1(9), 579–582.

Yoo, S.J., Seol, J.H., Shin, D.H., Rohrwild, M., Kang, M.-S., Tanaka, K. et al. (1996) Purification and characterization of the heat shock proteins HslV and HslU that form a new ATP-dependent protease in. *Journal of Biological Chemistry*, 271(24), 14035–14040.

Zhao, Z., Gonsior, M., Luek, J., Timko, S., Ianiri, H., Hertkorn, N. et al. (2017) Picocyanobacteria and deep-ocean fluorescent dissolved organic matter share similar optical properties. *Nature Communications*, 8(1),15284.

Zheng, Q., Chen, Q., Cai, R., He, C., Guo, W., Wang, Y. et al. (2019) Molecular characteristics of microbially mediated transformations of Synechococcus-derived dissolved organic matter as revealed by incubation experiments. *Environmental Microbiology*, 21(7), 2533–2543.

SUPPORTING INFORMATION

Additional supporting information can be found online in the Supporting Information section at the end of this article.

How to cite this article: Labban, A., Shibl, A.A., Calleja, M.L., Hong, P.-Y. & Morán, X.A.G. (2023) Growth dynamics and transcriptional responses of a Red Sea *Prochlorococcus* strain to varying temperatures. *Environmental Microbiology*, 25(5), 1007–1021. Available from: https://doi.org/10.1111/1462-2920.16326